ADVANCED FUNCTIONAL MATERIALS
www.afm-journal.de

Liquid Piezoelectric Materials: Linear Electromechanical Effect in Fluid Ferroelectric Nematic Liquid Crystals

*Marcell Tibor Máthé, Md Sakhawat Hossain Himel, Alex Adaka, James T. Gleeson, Samuel Sprunt, Péter Salamon, and Antal Jákli**

The first demonstration of converse piezoelectricity in 3D fluids is presented by measuring a linear electromechanical effect in ferroelectric nematic liquid crystals. The observed piezoelectric coupling constant below 6 kHz electric field is larger than 1 nC/N, comparable to, or better than, values for the strongest solid piezoelectric materials. Symmetry considerations indicate that the alignment of the ferroelectric nematic liquid crystal in the experimental study is not optimized, so the observed signal is likely only a fraction of the theoretically achievable signal. Understanding the electromechanical response of ferroelectric nematics will enable mechanical energy harvesting and open up a new avenue for developing fluid actuators, micro positioners, and electrically tunable optical lenses.

1. Introduction

Ferroelectric materials exhibit macroscopic, spontaneous electric polarization. This effect is only possible in materials that lack inversion symmetry. Such symmetry classes also permit *piezoelectricity*: linear coupling between electric field and mechanical deformations.[1] Piezoelectricity was discovered by the Curie brothers in 1880[2] in ferroelectric Rochelle salt. Ferroelectricity was subsequently observed in a number of other crystalline and/or solid materials, including ceramics,[3] and polymers.[4] Mesomorphic fluid materials, for example liquid crystal phases, may also lack inversion symmetry due either to molecular chirality, such as in ferroelectric chiral tilted smectic (SmC^*)[5,6] or chiral columnar[7] phases, or due to the polar shape of the molecules, such as in the case of bent-core molecules that form achiral polar smectic ($SmCP$) phases.[8] These examples do not represent true 3D fluids, as they possess positional order in one or two dimensions, and can therefore sustain some elastic strain. In contrast, nematic and cholesteric liquid crystals are fully fluid in three directions, i.e., their long-range order is purely orientational (and not positional). To date piezoelectricity in a nematic system has been observed only after cross-linking chiral molecules to produce a chiral nematic (N^*) elastomer.[9] In this case, while there is no long-range positional order, cross-linking severely restricts molecular motion resulting in the ability to sustain elastic strain.

Fluid ferroelectric nematic liquid crystals (FNLCs) were predicted to exist more than a century ago[10,11] but were only recently realized in practice.[12–18] FNLCs represent a highly desired and unique new phase of matter that combines true 3D fluidity with a high degree of polar order. Due to the macroscopic polarity, FNLCs lack inversion symmetry, which allows for several piezoelectric couplings that have to date remained unexplored.

In this paper, we will first discuss symmetry considerations and determine possible non-zero piezoelectric coupling constants of FNLCs. We then describe converse piezoelectric measurements on two room-temperature FNLC mixtures that demonstrate the first piezoelectric effects observed in liquids.

2. Symmetry Considerations

The *direct* piezoelectric effect (wherein electric polarization is induced via mechanical stress) can be mathematically expressed with:

$$P_i = \sum_{jk} \gamma_{i,jk} T_{jk} \tag{1}$$

where P_i is the polarization component induced by the stress tensor, T_{jk}, and $\gamma_{i,jk}$ is the third-rank piezoelectric coupling tensor. In

M. T. Máthé, P. Salamon
Institute for Solid State Physics and Optics
HUN-REN Wigner Research Centre for Physics
P.O. Box 49, Budapest H-1525, Hungary
M. T. Máthé
Eötvös Loránd University
P.O. Box 32, Budapest H-1518, Hungary
M. S. H. Himel, A. Adaka, A. Jákli
Materials Sciences Graduate Program and Advanced Materials and Liquid Crystal Institute
Kent State University
Kent, Ohio 44242, USA
E-mail: ajakli@kent.edu
J. T. Gleeson, S. Sprunt, A. Jákli
Department of Physics
Kent State University
Kent, Ohio 44242, USA
The ORCID identification number(s) for the author(s) of this article can be found under https://doi.org/10.1002/adfm.202314158

DOI: 10.1002/adfm.202314158

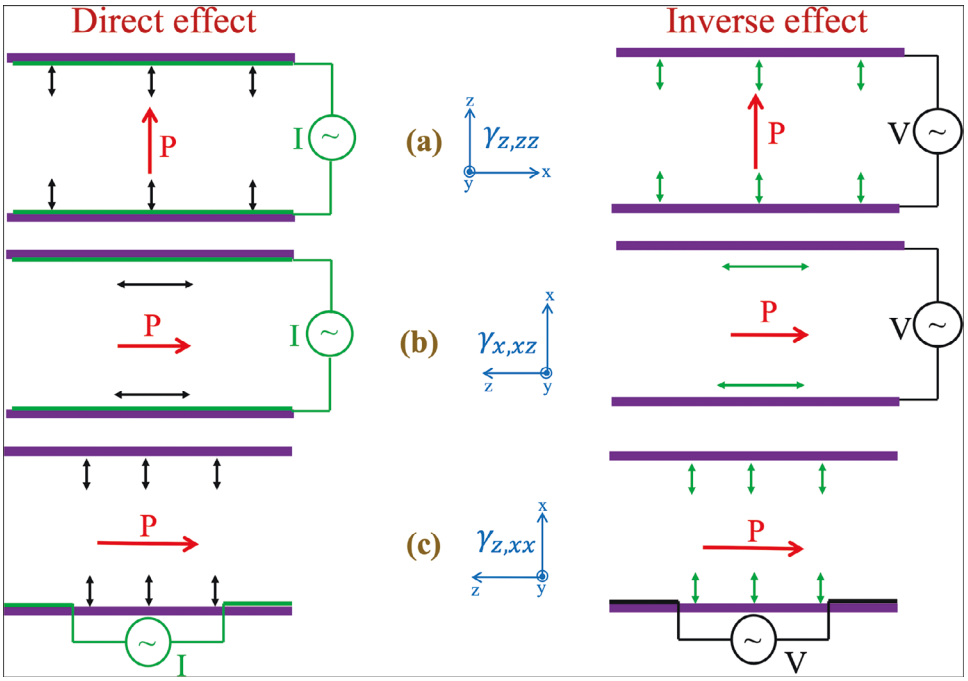

Figure 1. Possible experimental geometries that allow detection of direct and converse linear electromechanical (piezoelectric) signals in FNLC films. a–c) Geometries to detect $\gamma_{z,zz}$, $\gamma_{x,xz}$, *and* $\gamma_{z,xx}$, respectively. Left Column: Direct effect – Applying strain and measuring electric current; Right Column: Inverse effect – Applying electric voltage and measuring strain. Red arrows indicate the direction of the ferroelectric polarization (right-handed coordinate systems are chosen so that the ferroelectric polarization $\vec{P}$ is parallel to *z*). Black double headed arrows represent the applied strain for direct effect. Green double headed arrows show the electric field-induced strain for the converse effect.

the *converse* (or "inverse") piezoelectric effect, an applied electric field $\vec{E}$ results in material strain:

$$S_{jk} = \sum_{i} \gamma_{i,jk} E_i \tag{2}$$

where $\hat{S}$ is the strain tensor. Since *FNLC* materials are fluid, they cannot sustain steady shear or compression in any direction, i.e., the applied shear or electric field must be alternating, and the piezoelectric signals are expected to vanish at DC fields or during steady strain, as is the case in smectic and columnar piezoelectric liquid crystals along the fluid direction.[6]

The N_F phase has $C_{\infty v}$ symmetry, where C_∞ represents an infinite fold rotational symmetry about the polar axis, and the subscript v expresses a mirror symmetry through any plane containing the polar axis. Choosing the polar axis along *z*, any reflection through the $x-z$ (or $y-z$) plane changes the sign of y (or x), so all components of $\gamma_{i,jk}$ containing an odd number of either y or x, must be zero. Accordingly, there are only seven non-vanishing piezoelectric tensor elements: $\gamma_{z,zz}$, $\gamma_{z,xx}$($= \gamma_{z,yy}$) and $\gamma_{x,xz}$($= \gamma_{y,yz} = \gamma_{x,zx} = \gamma_{y,zy}$).[1] The first three elements permit a direct piezoelectric response along *z* as a result of a compression (extension) in either along or perpendicular to *z*. The last four non-vanishing elements indicate that a shear of a cylinder with axis along *z* would result in a radial polarization. When we consider converse piezoelectric response, the nonvanishing components dictate that compression/extension both parallel and perpendicular to *z* should result from an electric field applied along *z*. Applying field normal to the *z* would produce a shear flow along *z*. Note, for chiral ferroelectric nematic N_F^* phases,[19–21] the mirror plane is absent, C_∞ symmetry is obtained, and the above non-zero piezoelectric couplings exist without the equal signs.

All geometries we can expect piezoelectricity are shown schematically in **Figure 1**. Figure 1a–c shows the geometries to measure $\gamma_{z,zz}$, $\gamma_{x,xz}$, and $\gamma_{z,xx}$, respectively via direct and converse piezoelectric responses. Via the direct piezoelectric response, we measure the strain-induced polarization (P_S) current flowing through an electrode area Ω: $I_S = \Omega \cdot \frac{dP_S}{dt}$. In the converse piezoelectric responses, we measure the applied voltage-induced strain.

3. Results

We first studied two room temperature ferroelectric nematic liquid crystal materials (FNLC 1571 and FNLC 919) received from Merck in custom-made setups as shown in **Figure 2** and discussed in detail in the Materials and Methods section. FNLC 1571 films were studied using various driving frequencies between 10 Hz and 10 *kHz* and driving voltage from 0.1 V_{RMS} ($E_{RMS} \approx 4\frac{V}{mm}$) to 40 V_{RMS} ($E_{RMS} \approx 1.6$ V/μm). For voltages below 5 *V* ($E \approx 0.2\frac{V}{\mu m}$) at all measured frequencies, the original uniform polarizing microscopy texture (Figure 2a) remains unchanged. Above $E \approx 0.2$ $V/\mu m$, turbulent flows appeared below increasing frequencies at increasing voltages, such as below 500 Hz at $E \approx 0.2$ $V/\mu m$ and 3 kHz at $E \approx 0.8$ $V/\mu m$. Below $E \approx 0.6$ $V/\mu m$ the original texture reforms after removing the field. Increasing the voltage above $E \approx 0.6$ $V/\mu m$ a second harmonic (double frequency) vibration of

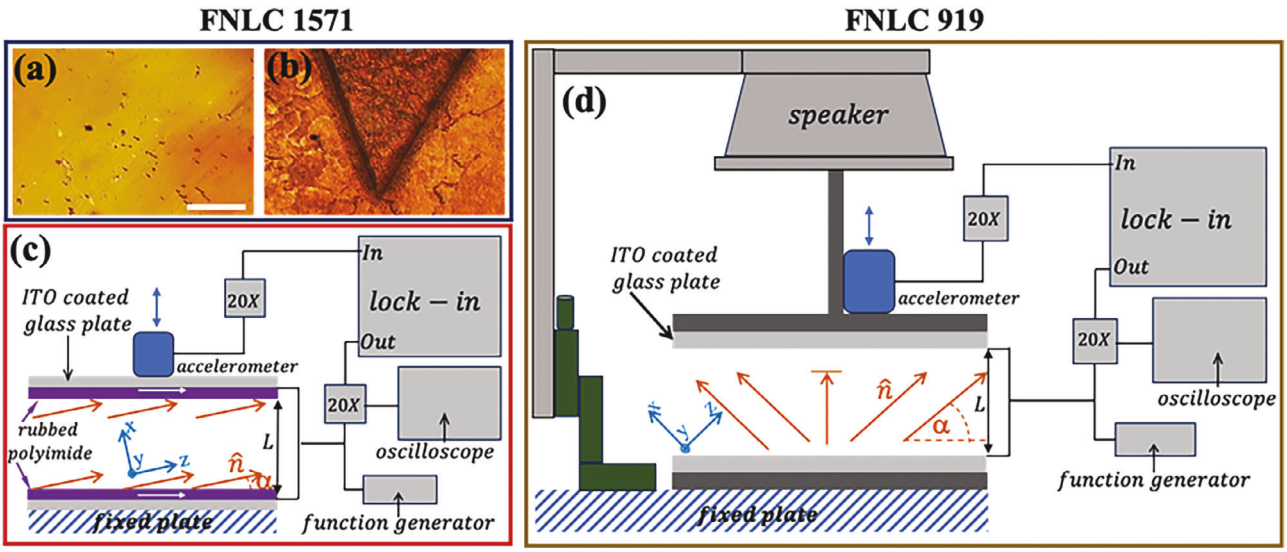

Figure 2. Schematic drawings showing typical Polarized Optical Microscopy (POM) textures of FNLC 1571, the director field ($\hat{n}$) of the studied films together with the custom-made setups. a,b) POM images of 24 μm FNLC 1571 samples below 5 V 100 Hz<f<10 kHz sinusoidal AC voltage signal applied between the ITO electrodes of the cover plates, and after 40 V, 10 Hz voltages, respectively. Scale bar represents 100 μm length. In (b) switching happens only within the darker triangle area indicating cracking of the ITO glass at the boundary of the triangle. c) Schematic drawing of the setup to study FNLC 1571 films with planar alignment coating resulting a pretilt α. As will be discussed in the Discussion section, $\alpha \approx 1°$, i.e., much smaller than indicated in the drawing. d) Schematic drawing of the custom-made setup to study FNLC 919 with the side-view of the director structure (Schlieren texture) as a result of the absence of the insulating alignment layer. This setup is capable to study both direct and converse piezoelectric responses at different temperatures.

the cell was observed to increase strongly due to electrostriction (Maxwell stress $\sigma = \epsilon_o \epsilon_r E^2$, where ϵ_o is the permittivity of the vacuum, ϵ_r is the relative dielectric constant, and E is the electric field applied). Such a double frequency vibration appeared to trigger unrepeatable signals, where the voltage dependence of the displacement at the base frequency is completely different during increasing and decreasing fields. Above $E \approx 1.6\ V/\mu m$ the device is irreparably damaged due to zig-zag shaped cracks forming in the ITO layer, as shown in Figure 2b. Such ITO cracking also damaged the polyimide alignment layer causing permanently inhomogeneous alignment.

On the other hand, when the maximum amplitude of the voltage is less than 10 V, the signals are identical under increasing and decreasing fields, and the voltage dependence is linear, as shown in **Figure** 3a on a fresh 24 μm FNLC 1571 sample and in Figure 3b for a 100 μm FNLC919 film. Based upon these observations, the results described here only reflect driving voltages below 10 V.

The vibration amplitude A_f was measured at the applied frequency f with an accelerometer connected to the vibrating bounding plate. The frequency dependence of A_f is shown in Figure 3c for a 24 μm FNLC 1571 for both increasing and decreasing frequencies, and for a 100 μm FNLC 919 sample at increasing frequencies. The most important features for both samples are the decrease of A_f from $\approx 100\ nm$ at 100 Hz to $\approx 0.2\ nm$ at $3kHz$, then remaining basically constant up to 6 kHz where the measurement concluded. Strikingly, A_f of the 100 μm FNLC 919 is roughly ten times larger, yet the frequency trend is similar to the 24 μm FNLC1571 sample. Also seen are a few frequency peaks likely due to normal modes of the apparatus (e.g., glass plates and/or mechanical assemblies). More peaks are seen in the FNLC 919 sample, as this was measured in a reconfigured apparatus shown in Figure 2d having apparently more normal modes.

These measurements of A_f demonstrate linear coupling between the external electric field and mechanical deformation of the ferroelectric nematic liquid crystals, i.e., a linear electromechanical effect. This response is only possible via the converse piezoelectric effect predicted in Equation 2. The strain, S, in the present geometry is the ratio of the amplitude of the vibration Δx to the film thickness L ($S = \Delta x / L$) while the applied electric field is $E \approx U/L$, giving the measured piezoelectric coupling constant (also called piezoelectric charge constant) as $\gamma = \Delta x/U$. Using the data visualized in Figure 2c, we determined that the maximum measured coupling constant below 400 Hz is $10^{-7}\ m/5V = 2 \times 10^{-8}\ m/V$ (C/N) and 3×10^{-7} m/5 V $= 6 \times 10^{-8}\ m/V$ for FNLC 1571 and FNLC 919, respectively. The high frequency (above 1 kHz) values are $\approx 10^{-10}$ and $2 \times 10^{-9}\ m/V$ for FNLC 1571 and FNLC 919, respectively. At higher frequency values, the piezoelectric coefficient is comparable with the highest values found so far in crystals,[22,23] in cellular polymers (ferroelectrets),[24] or soft composite fiber mats.[25] Here we note that recently a "piezoelectric" effect with $\approx 3 \times 10^{-13}\ m/V$ was reported for an ionic liquid.[26] However, since that fluid is isotropic with centrosymmetry, by definition, it cannot be considered a piezoelectric effect that requires a lack of inversion symmetry.

The linear electromechanical response decreases with increasing temperature (with room temperature being the minimum attainable with this apparatus) to being essentially immeasurable upon transition to the (non-ferroelectric) ordinary nematic phase, as seen in Figure 3d. This clearly shows that this

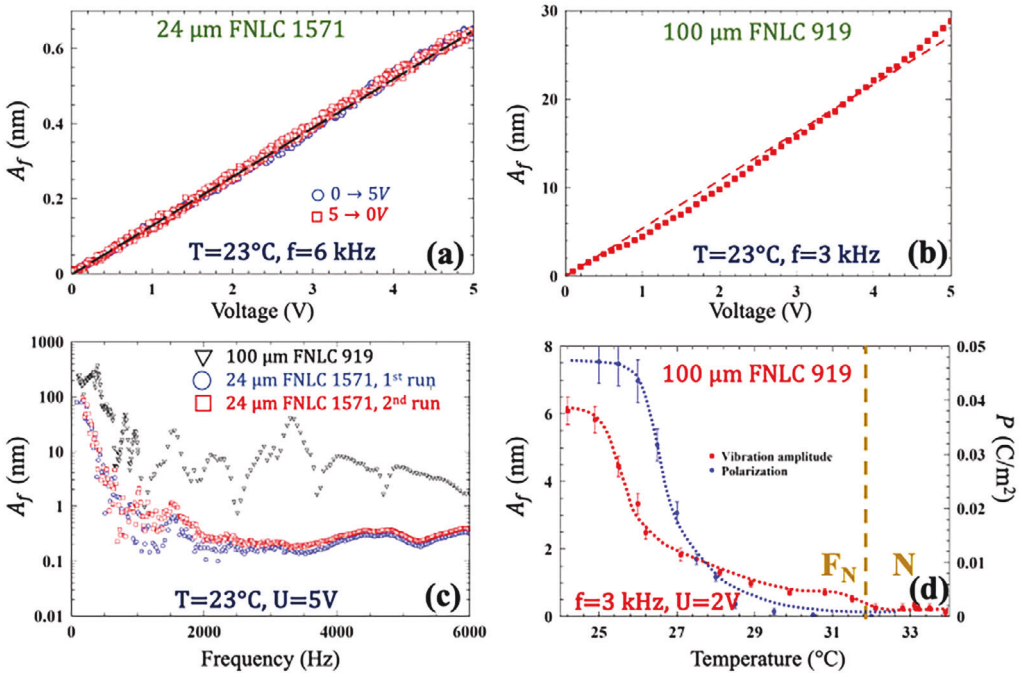

Figure 3. Amplitude A_f of periodic vertical vibrations of the horizontal top plate at the frequency of the applied field under various conditions. a,b) Room temperature voltage dependence of A_f of a 24 μm thick FNLC 1571 sample at $f = 6\ kHz$ and of a 100 μm FNLC 919 at $f = 3\ kHz$, respectively. c) Frequency dependence of A_f under 5 V amplitude applied voltage for 100 μm FNLC 919 (black triangle) and for a 24 μm FNLC 1571 film at first run (blue circle) and during second run (red square). d) Temperature dependence of A_f when $U = 2\ V_{rms}, f = 3kHz$ sinusoidal voltage applied between the ITO coated glass plates (left axis) and the temperature dependence of the ferroelectric polarization plotted against the right axis.

linear electromechanical effect is a property only of the ferroelectric nematic phase. We note that the strong decrease of the piezoelectric signal at 27 °C (≈5 °C below the $N_F - N$ transition) is likely related to the presence of the multiple components of the FNLC 919 mixture and is paralleled by a strong decrease of the ferroelectric polarization at 27°C that is plotted in Figure 3d against the right y-axis.

We also note that the piezoelectric effect is sufficiently pronounced, especially in the $3 - 6\ kHz$ range, as to be clearly audible! Such audible electromechanical responses were also detected by ear at the frequency of the applied voltages even for single component high temperature FNLC's such as RM734[12] and DIO,[13] indicating that this linear electromechanical effect is a general property of all FNLCs.

In **Figure 4**, we plot the time dependence of the acceleration of the vibrating plate for various frequencies.

Figure 4a–d shows the time dependence of the acceleration of a 24 μm FNLC 1571 sample at 10 V, 100 Hz square wave voltage, at 500 Hz, 3 kHz and 5 kHz 7 V_{RMS} sinusoidal voltages, respectively. Well below 1 kHz, we found transient vibrations for both square wave (see Figure 4a) and sinusoidal (see Figure 4b) applied voltages that are generated during field reversals. These vibrations have a natural frequency of ≈18 kHz and decay time of ≈1 ms. These transient vibrations are likely related to director rotation induced flow which triggers an elastic deformation of the bounding glass, and which is damped by the viscous FNLC film. Due to the 1 ms decay time, this mode cannot be effectively generated well above 1 kHz as can be seen in Figure 4c,d, where the response becomes essentially sinusoidal with the frequency of the applied voltages, corresponding to purely linear electromechanical signals.

The range of the linear electromechanical response depends strongly on the magnitude of the applied field. This is illustrated in Figure 4e,f for a 100 μm FNLC 919 sample under 3 kHz applied voltages. While the mechanical response is purely linear at $U \approx 2\ V_{rms}$, a second harmonic signal corresponding to electrostriction is observed at $U \approx 5\ V_{rms}$.

Comparing the waveforms of the FNLC 1571 and FNLC 919 samples, we found that the linearity observed at lower frequencies and at higher voltages for the FNLC 1571 than of FNLC 919. This is likely related to the different viscosities, namely that in FNLC 1571 the rotational viscosity measured to be $\approx 1.6\ Pa \cdot s$ while for FNLC 919 it was found to be only $\approx 0.75\ Pa \cdot s$, so the director rotates much less under the same conditions in FNLC 1571 than in FNLC 919.

4. Discussion

How to understand the context of these measurements with the phenomenon as envisaged in the introduction, the differences between the two materials that were examined, and the issue of what is the maximum achievable converse piezoelectric performance in this entirely new class of materials? It is instructive to compare the ideal geometries as depicted in Figure 1 with the actual embodiment assembled in the laboratory as shown in Figure 2c,d for the FNLC 1571 and FNLC 919, respectively. Figure 1 shows that in planar alignment one would expect zero

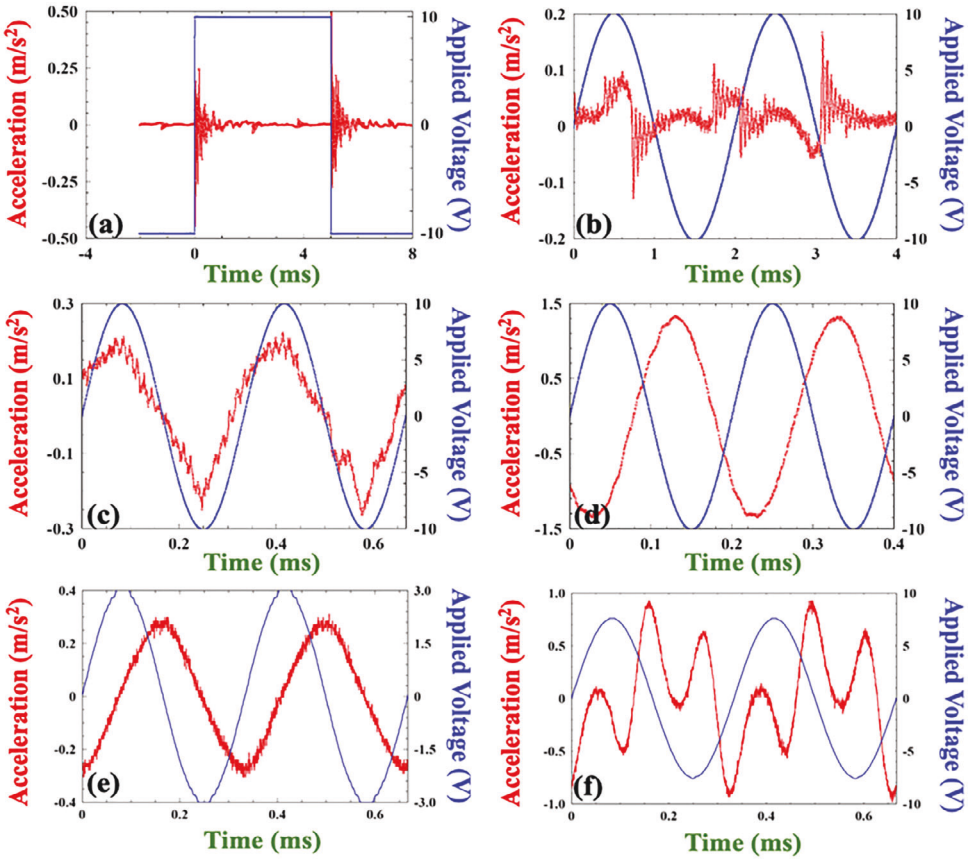

Figure 4. Time dependences of the applied voltage (blue lines, plotted against the right axes) and of the acceleration of the cover plate (red line, plotted against the left axes) of a 24 µm FNL 1571 sample at a) 0.1 kHz, b) 0.5 kHz, c) 3 kHz, and d) 5 kHz, and for a 100 µm FNLC 919 sample at 3 kHz of e) $U \approx 2V_{RMS}$ and f) $U \approx 5V_{RMS}$.

converse piezoelectric vibration normal to the substrates because this would entail the tensor element $\gamma_{x,xx}$, which is zero by symmetry. Symmetry allows piezoelectricity only when there is a component of the polarization along the field, i.e., when $\gamma_{z,zz}$ becomes effective. In fact, ideal planar alignment, where the optical axis is exactly in the $y-z$ plane has never been achieved in construction of liquid crystal cells. In practice, one always obtains planar alignment having a "pre-tilt" angle, α, between the optic axis (which is the direction of polarization) and the plane of the electrode which provides a vertical component of the polarization, $P_v = P_o\, sin\alpha$. The minimum pretilt that is sufficient to provide the observed effect can be estimated from the ratio of the mechanical energy to the supplied electrical energy, which should be less than 1. The mechanical energy can be estimated from the kinetic energy $W_k = \frac{1}{2}\, m\, v^2 = \frac{1}{2}\, m(A_f 2\pi f)^2$, where $m \approx 10g$ is the mass of the top glass and of the accelerator, f is the frequency of the applied field and A_f is the measured base frequency amplitude. The electric energy is $W_E = P_o\, sin\alpha \cdot E \cdot V$, where $E \approx \frac{U}{L}$ and $V = \Omega \cdot L$ is the volume of the sample, and Ω is the area of the film with thickness L. The smallest pretilt α_{min} then can be calculated as $\alpha_{min} = sin^{-1}(\frac{m(A_f 2\pi f)^2}{2P_o U\Omega})$. From Figure 3c, and taking $P_o = 3 \cdot 10^{-2}\frac{C}{m^2}$, $A_f \approx 400\, nm$ at $f = 300\, Hz$, $U = 5V$ and $\Omega = 1\, cm^2$ for FNLC 919, we get $\alpha_{min} = 0.01°$. Realistically of course, the piezoelectric coupling factor should be much smaller than 1 (perhaps a few percentages), so the pretilt should be much larger than 0.01°. The pretilt for ferroelectric nematic liquid crystals with insulating planar alignment as for FNLC 1571, is likely to be small due to the depolarization field $E_{dep} = -\frac{P_o sin\alpha}{\epsilon \cdot \epsilon_o}$ that tends to realign the polarization along the substrate.[14] In practice, the pretilt is limited by the charge density of the free ions ϱ_i that can balance the depolarization charge density $P_o sin\alpha$. This gives for a charge density of the ions $\varrho_i = \frac{P_o sin\alpha}{L} < \frac{3\cdot 10^{-2}\cdot 10^{-2}}{10^{-4}} \approx 3\frac{C}{m^3}$. Assuming monovalent ions with number density n_i and charge mobility µ, the conductivity of the FNLC sample is $\sigma = qn_i\mu = \varrho_i\,\mu$. The Einstein–Smoluchowski equation relates the charge mobility to the diffusion coefficient D and the temperature T in Kelvin as $\mu = \frac{qD}{k_B T}$, where $k_B = 1.38 \cdot 10^{-23} J/K$. With $D \approx 10^{-11}\frac{m^2}{s}$, $q = 1.6 \cdot 10^{-19}\ C$ and $T = 300\ K$, we get for the electric conductivity that $\sigma = \varrho_i \frac{qD}{k_B T} < \frac{3\cdot 1.6\cdot 10^{-19}\cdot 10^{-11}}{1.38\cdot 10^{-23}\cdot 300} \approx 10^{-9}(\Omega m)^{-1}$. Indeed, we measured that the conductivity of FNLC 1571 is $\approx 10^{-8}\ (\Omega m)^{-1}$, thus allowing a pretilt of $\geq 1°$. In the FNLC 919 samples without insulating alignment coating, Schlieren textures were obtained and the angle α between the bounding plate and the ferroelectric polarization would be estimated as significantly larger (see Figure 2d). In these circumstances, one would naturally expect to measure a larger converse piezo-electric response, which we

indeed found as the results in Figure 3c show the vibration amplitude of FNLC 919 is at least one order of magnitude larger than in FNLC 1571.

The obvious step would be to perform this experiment in homeotropic geometry, where the polarization direction is parallel to the displacement. However, this geometry is particularly difficult to achieve as it induces a depolarization field which inhibits the desired alignment. In principle, achieving homeotropic alignment or increasing the pre-tilt angle potentially allows for a dramatic (perhaps ten or hundred times) augmentation of the electromechanical effects we report here.

5. Conclusion

We have observed and analyzed linear electromechanical effects, corresponding to converse piezoelectricity, in two room temperature liquid ferroelectric nematic liquid crystals. The observed piezoelectric coupling constant (which represents only a lower limit of the constant due to the weight of the connected sensors and other components) found to be comparable to or exceed that of the strongest solid piezoelectric materials. Our analysis indicates that the observed effect is due to $\gamma_{z,zz}$ and a small pretilt or electric field induced realignment of the molecular orientation, therefore it is far from the optimum configuration to obtain the maximum piezoelectric signal. Future experiments will concentrate on the geometry shown in Figure 1c to achieve higher piezoelectric signal. We will also explore the direct piezoelectric effects for the geometries shown in the right column of Figure 1a–c both for achiral and chiral ferroelectric nematic liquid crystals. Even though a number of further experiments are possible and needed, our initial observation is significant, since linear electromechanical coupling is an inherent property of ferroelectric materials, but so far has only been explored in crystals, polymers, and positionally ordered liquid crystals.

Understanding the electromechanical response of nonchiral and chiral ferroelectric nematics will enable mechanical energy harvesting, and lead to novel fluid actuators, micro positioners, and electrically tunable optical lenses.

6. Experimental Section

The converse piezoelectric signals of two room temperature ferroelectric nematic mixtures (FNLC 1571 and FNLC 919) were studied, provided to us by Merck. FNLC 1571 had two nematic phases N_1 and N_2 above the ferroelectric nematic N_F phase. The phase sequence in cooling was I 88 °C N_1 62 °C N_2 48 °C N_F 8 °C Cr. FNLC 919 had two nematic phases, N and N_1 above the N_F phase with the phase sequence in cooling as I 80 °C N_1 44 °C N 32 °C N_F 8 °C Cr. FNLC 919 was studied by Yu et al[27] and Máthé et al[28] and the ferroelectric polarization was measured in free-standing threads at room temperature to be $P_o \approx 3 \cdot 10^{-2}$ C m^{-2}.[28] This value was smaller than the $P_o \approx 4.7 \cdot 10^{-2}$ C m^{-2} ,in in-plane field geometry (see Figure 3d) were measured here, likely due to the inhomogeneous field in the free-standing threads.[28]

Both FNLCs were contained between two, parallel glass plates having conducting indium tin oxide (ITO) sputtered in their inner surface, separated by a distance d, which was much smaller than the lateral dimensions ($1 - 2$ cm) of the planes.

In case of FNLC 1571, the bounding conducting surfaces were overcoated by a uniformly rubbed polyimide (PI2555) layer that aligns the director parallel to the surface and the rubbing direction, called *planar* alignment. The substrates were separated only by $L = 24$ μm thick liquid crystal film, held in place solely by surface tension. After the FNLC was filled by capillary action, an accelerometer (Brüer & Kjaer, model BK4375, mass: 2.4 g excluding cable, charge sensitivity: $i_s = 0.32$ $pA/(ms^{-2})$, voltage sensitivity: $v_s = 0.61$ $mV/(ms^{-2})$) was fixed to the top plate.

In case of FNLC 919, the conducting surfaces were not treated by any alignment layer and the alignment was not uniform, but rather adopted the 'Schlieren" texture, where director $\hat{n}$ exhibits a roughly constant angle with respect to the plates and was degenerate in the plane of the bounding planes. FNLC 919 was studied using a slightly different setup shown in Figure 2d. There the lower glass substrate was fixed in place, and the upper plate was connected to an electrically actuated diaphragm that allowed movement in vertical direction; the upper plate also held the same BK4375 accelerometer. Although, here in this study the converse effect was only measured, this setup was designed so that it could measure the direct piezoelectric response as well. The gap between the glass plates was adjustable by micro-positioners and measured via microscope. For the measurements reported here, the gap was set to 100 μm and the upper plate's acceleration was measured.

For both LC materials the voltage developed by the accelerometer (V_{acc}) was measured using a lock-in amplifier (Stanford Research Systems, model SR830), so that the internal reference signal of the lock-in amplifier provides the applied voltage. With the lock in amplifier, the amplitude A and phase ϕ of the time-dependent acceleration were measured at the reference frequency f and at $2f$. At the base frequency $A_f = a/(2\pi f)^2$, whereas at $2f$, $A_{2f} = a/(8\pi f)^2$, where $a = V_{acc}/v_s$ was the acceleration of the plate. The accelerometer signal induced by rectangular and sinusoidal voltages applied by a function generator was also monitored via an oscilloscope to examine non-harmonic contributions.

The temperature dependence of the ferroelectric polarization and the rise times of FNLC 1571 and 919 were measured under 80 Hz triangular electric waveforms in 10 µm thick cells with $d(FNLC\ 1571) = 1\ mm$ and $d(FNLC\ 919) = 0.5\ mm$ gap between in-plane ITO electrodes, as described in references.[14,19,29] The approximate rotational viscosity (γ_1) values were determined from the rise time τ as $\gamma_1 \approx \tau \cdot P \cdot \frac{U}{d}$, where U is the applied voltage. At 25°C $P = 6.3 \cdot 10^{-2}$C m^{-2} $\tau \approx 260$ µs at $U = 90V$ were obtained for FNLC 1571, and $P = 4.7 \cdot 10^{-2}$C m^{-2} $\tau \approx 150$ µs at $U = 60V$, giving rotational viscosities of 1.6 $Pa \cdot s$ and 0.75 $Pa \cdot s$ for FNLC 1571 and FNLC 919 materials.

Statistical Analysis: In each measurement, the reproducibility and reliability of the observations were tested. In case of measurement with oscilloscope, eight times averaging of the instrument to increase the signal/noise ratio were used. For the measurements with lock-in amplifier, 2 s integration time was used. This means averaging by $N = 2 \cdot f$ times, where f is the frequency.

Acknowledgements

This work was financially supported by US National Science Foundation grant DMR-2210083 and by the Hungarian National Research, Development, and Innovation Office under Grant NKFIH FK142643 and EIG CONCERT-Japan project FerroFluid (P.S.). P.S. was supported by the János Bolyai Research Scholarship of the Hungarian Academy of Sciences. The materials FNLC 1571 and FNLC 919 were provided by Merck Electronics KGaA, Darmstadt, Germany.

Conflict of Interest

The authors declare no conflict of interest.

Data Availability Statement

The data that support the findings of this study are available from the corresponding author upon reasonable request.

Keywords

ferroelectric nematic, liquid electromechanics, piezoelectricity

Received: November 10, 2023
Revised: December 21, 2023
Published online:

[1] L. D. Landau, E. M. Lifshitz, *Electrodynamics of Continuous Media - Volume 8 of Theoretical Physics*, 2nd ed., Pergamon Press, Oxford **1984**.
[2] J. Curie, P. Curie, *Bulletin de la Société minérologique de France*, Imprimerie De A. Masson, LAMANON **1880**, *3*, 294.
[3] S. Roberts, *Phys. Rev Lett.* **1947**, *71*, 890.
[4] E. Fukada, *IEEE Trans. Ultrason Ferroelectr. Freq. Control* **2000**, *47*, 1277.
[5] A. Jákli, L. Bata, Á. Buka, N. Éber, I. Jánossy, *J. Physique Lett.* **1985**, *46*, 759.
[6] A. Jákli, *Liq. Cryst.* **2010**, *37*, 825.
[7] A. Jakli, M. Muller, D. Kruerke, G. Heppke, *Liq. Cryst.* **1998**, *24*, 467.
[8] A. Jákli, I. C. Pintre, J. L. Serrano, M. B. Ros, M. R. De La Fuente, *Adv. Mater.* **2009**, *21*, 3784.
[9] W. Meier, H. Finkelmann, *Macromolecules* **1993**, *26*, 1811.
[10] M. Born, *Sitzungsber. Preuss Akad. Wiss* **1916**, *30*, 614.
[11] O. D. Lavrentovich, *Proc. Natl. Acad. Sci. U.S.A.* **2020**, *117*, 14629.
[12] R. J. Mandle, S. J. Cowling, J. W. Goodby, *Phys. Chem. Chem. Phys.* **2017**, *19*, 11429.
[13] H. Nishikawa, K. Shiroshita, H. Higuchi, Y. Okumura, Y. Haseba, S.-I. Yamamoto, K. Sago, H. Kikuchi, *Adv. Mater.* **2017**, *29*, 1702354.
[14] X. Chen, E. Korblova, D. Dong, X. Wei, R. Shao, L. Radzihovsky, M. A. Glaser, J. E. Maclennan, D. Bedrov, D. M. Walba, N. A. Clark, *Proc. Natl. Acad. Sci. U.S.A.* **2020**, *117*, 14021.
[15] N. Sebastián, M. Copic, A. Mertelj, *Phys. Rev. E* **2022**, *106*, 021001.
[16] R. J. Mandle, N. Sebastián, J. Martinez-Perdiguero, A. Mertelj, *Nat. Commun.* **2021**, *12*, 4962.
[17] N. Sebastián, L. Cmok, R. J. Mandle, M. R. De La Fuente, I. Drevensek Olenik, M. Copic, A. Mertelj, *Phys. Rev. Lett.* **2020**, *124*, 037801.
[18] A. Mertelj, L. Cmok, N. Sebastián, R. J. Mandle, R. R. Parker, A. C. Whitwood, J. W. Goodby, M. Čopič, *Phys. Rev. X* **2018**, *8*, 041025.
[19] C. Feng, R. Saha, E. Korblova, D. Walba, S. N. Sprunt, A. Jákli, *Adv. Opt. Mater.* **2021**, *9*, 2101230.
[20] X. Zhao, J. Zhou, J. Li, J. Kougo, Z. Wan, M. Huang, S. Aya, *Proc. Natl. Acad. Sci. U.S.A.* **2021**, *118*, e2111101118.
[21] J. Ortega, C. L. Folcia, J. Etxebarria, T. Sierra, *Liq. Cryst.* **2022**, *49*, 2128.
[22] D. Tanaka, T. Tsukada, M. Furukawa, S. Wada, Y. Kuroiwa, *Jpn. J. Appl. Phys.* **2009**, *48*, 9KD08.
[23] H. Cao, H. Luo, *Ferroelectrics* **2002**, *274*, 309.
[24] S. Bauer, R. Gerhard-Multhaupt, G. M. Sessler, *Phys. Today* **2004**, *57*, 37.
[25] J. Morvan, E. Buyuktanir, J. L. West, A. Jákli, *Appl. Phys. Lett* **2012**, *100*, 063901.
[26] M. I. Hossain, G. J. Blanchard, *J. Phys. Chem. Lett.* **2023**, *14*, 2731.
[27] J.-S. Yu, J. H. Lee, J.-Y. Lee, J.-H. Kim, *Soft Matter* **2023**, *19*, 2446.
[28] M. T. Máthé, K. Perera, Á. Buka, P. Salamon, A. Jákli, *Adv. Science* **2024**, 2305950, https://doi.org/10.1002/advs.202305950.
[29] R. Saha, P. Nepal, C. Feng, M. S. Hossain, M. Fukuto, R. Li, J. T. Gleeson, S. Sprunt, R. J. Twieg, A. Jákli, *Liq. Cryst.* **2022**, *49*, 1784.